Development and Experimental Investigation of Portable Solar-powered Thermoelectric Cooler for Preservation of Perishable Foods

Olipriya Biswas*[,1], Palani Kandasamy*‡

*Department of Agricultural Engineering, Institute of Agriculture, Visva-Bharati (A Central University), Santiniketan, West Bengal 731235, India

[1]Department of Fishery Engineering, Faculty of Fishery Sciences, West Bengal University of Animal & Fishery Sciences, Kolkata 700094, India

(olipriya.online16@gmail.com, pkandasamy1973@gmail.com)

‡Corresponding author; Palani Kandasamy, Department of Agricultural Engineering, Institute of Agriculture, Visva-Bharati, Santiniketan, West Bengal 731235, India. Tel: +91-9434306277, pkandasamy1973@gmail.com

Received: 25.06.2021 Accepted: 06.08.2021

Abstract- Preservation of perishable foods is a major issue where inconsistent electricity supply. In this study, a solar thermoelectric cooler (STEC) was fabricated by exploiting the solar energy and evaluated its cooling performance with and without product load. The STEC comprised of a thermoelectric module (TEM), inner and outer heat sink-fan fixed in the cooler box wall, and photovoltaic (PV) panel connected with the device through battery and PV charge controller. The PV power utilized to drive the device, charge the battery in the daytime, and the store electricity exploited during night time. The effect of varying input electric current on the cold side temperature of TEM, cooling capacity, power consumption and coefficient-of-performance (COP) were investigated. The results showed that the cold side temperature decreased to 5±0.2ºC in 120 and 180 min for without and with product load (0.5 kg fish fillets), respectively. The cooling capacity, power consumption and COP of the STEC were 23.8 W, 53.5 W and 0.44, respectively, at the input electric current of 3.5 A. The battery power was utilized to drive STEC for 5-6 h after sunset. The STEC could be considered as an alternate "green-option" to the domestic refrigerator where electricity is not accessible.

Keywords Solar photovoltaic system, thermoelectric module, power consumption, cooling capacity, COP.

1. Introduction

Refrigeration demand is increasing worldwide, mainly for food preservation, medical services, automobile and household airconditioning, cooling of electronic and scientific instruments [1-3]. The vapour compression and vapour absorption refrigeration systems are widely used for domestic and industrial purposes due to their high coefficient-of-performance (COP); however, they consume high electric power, uses liquid refrigerants which have negative environmental impacts, and not easy to develop as portable and lightweight devices for outdoor use [4,5]. The large size of the vapour compression refrigerator limits its application in small and temporary places [6]. Thermoelectric cooling systems (TECS) have many advantages over other systems, in fact, no irreversible harm to the environment, rapid thermal response, noiseless, compact in size, lightweight, portable, high reliability, low-cost production, less maintenance, long lifetime, viable for outdoor use combined with solar photovoltaic cells, and attractive to use as mini-refrigerator for preserving foods and drugs in small places [6,7]. The TECS are widely used to cool laboratory equipment, thermal sensors in scientific equipment, computer equipment, and water cooling, low capacity cooling devices for domestic and industrial purposes [8]. However, there is a limitation to the TECS that too low COP even less than one [4].

Refrigeration energy is a big issue where inconsistent supply of electricity and difficult to get conventional fuels. Solar energy is the adequate solution for today and long term energy crises and important green resource because of its flexibility, simplicity and abundant supply of energy. The solar energy is an excellent option to generate clean electricity, and it has been exploited for different domestic and engineering applications [9-14]. Solar refrigeration could be an alternative to conventional refrigerators. In a solar refrigeration system, solar energy is converted into electrical energy by photovoltaic (PV) technology, utilized to drive the refrigeration systems [15]. Though the intensity of solar radiation varies with time, the cooling potential of the solar refrigeration system becomes maximum during the time of sunshine supply [16]. Thus it has been recommended as green cooling technology, especially in hot regions, where inconsistent supply of electricity and a great amount of solar energy available [5].

The TECS works based on the principles of the Peltier effect, briefly, pairs of n- and p-type semiconductor thermoelements (n-type has excess electrons whereas p-type has deficit), connected electrically in series and thermally in parallel, interconnected by copper strips, integrated thermally conducting ceramic plates on each side. When a DC flows across the junction of the semiconductors, one side will be cooled, whereas the other is heated depending on the direction of the current. If electrons flow from p-type to n-type, heat is absorbed in the n-type side due to electrons jumping towards a higher energy state. The heat absorbed at the cooling side is transferred to the other side, becomes hot [17]. A single-stage thermoelectric module can transfer heat at a rate of 125 W or can accomplish a temperature difference up to 70°C [18]. The Peltier effect converts the input electric current into a temperature gradient, and heat transfer occurs from heat source to heat sink by electrons; thus, the system does not require any refrigerant [8].

In the past years, various research on the TECS has been carried out to enhance thermoelectric performances, energy efficiency, and optimum working conditions. Aboelmaaref et al. [5] illustrated that the cooling capacity and COP of thermoelectric air-conditioning system driven by solar photovoltaic panel 30 W and 2.2, respectively at a design point with an input current of 2.5 A, which suitable for saving energy. Chen et al. [7] reported that the cooling capacity and COP of the thermoelectric chiller driven by the direct current and solar cell were 11.9 W, 11.2 W and 0.35, 0.74, respectively, indicating solar-driven was significantly better than driven by direct current. Daghigh and Khaledian [8] demonstrated that the operation time, energy consumption and COP of compression cooling system and thermoelectric hybrid cooling system were 16,380 s, 8636.8 kJ and 5.3 and 15,000 s, 7911 kJ and 5.4, respectively, indicating a better performance for the hybrid cooling system.

Dai et al. [16] reported that the temperature of thermoelectric refrigerator driven by solar photovoltaic cells was ranging from 5ºC to 10ºC, and experimental COP was 0.36. Min and Rowe [19] demonstrated that the COP of thermoelectric refrigerator was around 0.3-0.5 at an operating temperature of 5ºC and an ambient temperature of 25ºC. Abdul-Wahab et al. [20] Observed that the temperature of solar thermoelectric refrigerator declined to 5ºC from 27°C in 45 min, and the COP of the device was about 0.16.

Cheng et al. [21] investigated the cooling efficiency of the solar-driven thermoelectric module for green building applications. They found that the module was built a temperature difference of 16.2ºC between the model house and ambient. He et al. [22] reported that the temperature of a model room (0.125 m^3) was reached to 17ºC at summer time and the COP of the thermoelectric cooling system driven by solar cells was higher than 0.45. Ohara et al. [23] reported that the portable thermoelectric vaccine refrigeration system achieved a minimum temperature of 3.4ºC and diminished power consumption by 50% when it reached twice the temperature difference.

Gökçek and Şahin [24] reported that the COP of mini channel water-cooled thermoelectric refrigerator was 0.19 and 0.23 for the flow rate 0.8 L/min and 1.5 L/min, respectively, at the end of 25 min and the corresponding inner temperatures of the refrigerator were 2ºC and -0.1ºC. Atta [25] studied solar thermoelectric cooling using closed-loop heat exchangers with macro channels and reported that the system was cooled a closed room space of 30 m^3 by 14°C within 90 min COP of 0.72 when the PV input current at 11.2 Å and 12 V. Batra et al. [26] reported that the temperature of thermoelectric refrigerator was dropped by 6.7ºC and 8.6ºC under natural and forced cooling mode, respectively.

In the literature, most of the research focused on utilising the integrated PV/thermoelectric systems for room air-conditioning, water tank cooling and space cooling. Besides, most of these studies used conventional electrical power to drive TECS. However, the research on portable solar-powered thermoelectric cooling systems for preserving perishable foods in the literature was very few [7,16,20] and showed the COP of less than 1.0. Hence, intensive research on the solar thermoelectric cooling systems needs to enhance its COP. There are no ready-made, user-friendly solar thermoelectric cooling appliances for the retail fruits, vegetables, drinks, and fish sellers in the remote and rural areas in India. This has particularly prompted to formulate the present investigation on the development of a portable, cost-effective solar thermoelectric cooler. The present investigation objectives were (i) to design and fabricate a portable, cost-effective solar-PV powered thermoelectric cooler (ii) to investigate the cooling capacity and COP of the fabricated thermoelectric cooler.

2. Materials and Methods

2.1. Sample preparation

The cooling performance of the fabricated solar thermoelectric cooler (STEC) tested under hot weather conditions (during April-May 2019) of Santiniketan (23°40'N, 87°41'E), West Bengal, India. The average outside temperature was in the range of 30-34°C during this period. In this work, chillness of fish fillets stored in the STEC was tested, thus the fresh samples of about 0.5 kg kept in the

STEC. The following procedure was adopted while preparation of fish fillet samples. Freshly harvested basa fish were purchased from a local fish farm, stunned by applying a blow on the skull with a hammer, then slaughtering and bleeding of fish were done by cutting the gill arches and main blood vessel from the heart with a sharp knife. Then the fish were scaled, beheaded, gutted, washed with water, filleted, and packed in a low-density polyethene pouch.

2.2. Description of experimental setup

The portable STEC consists mainly of a cooler box, solar-PV module, power storage battery, thermoelectric module, heat sinks, and fans. The cooler box is a roto-moulded plastic container made up of food-grade double tough high-density polyethene (HDPE), each 6 mm thick, and a refrigeration grade polyurethane insulation foam layer of 50 mm thick filled in the double tough wall construction. The internal dimension of the cooler box is 0.36×0.28×0.25 m (length × width × height) with a volume of 0.0252 m^3. A stretch hold down loops having a constant pressure mechanism used for closing the lid. Thermal conductivities of HDPE and polyurethane foam insulation materials are 0.44 and 0.028 W/mK, respectively. The insulation is used to inhibit the backflow of heat and prevent any loss in the cooler's performance affected by external heat. The estimated total heat energy in the experimental cooler box was 41.52 W (Eq. 6). The cooler box used in this study was purchased from the Aristoplast Products Pvt. Ltd, Mumbai, India.

A polycrystalline type solar-PV module with an actual power output rating of 100 W_p, efficiency of 13.2%, and size of 1032 × 672 mm was used in this study. The PV module size is based on the power requirement of the thermoelectric cooler and other factors (Eq. 24). The PV module was supplied by Vinova Energy Systems Private Limited, Tamil Nadu, India. The electrical power generated by the PV module was utilized to drive the thermoelectric cooler directly. A tubular type lead-acid battery with a storage capacity of 80 Ah was used to store the electrical power of the PV module, and store electricity can be exploited during night time. The battery capacity was chosen based on power for thermoelectric cooler, battery efficiency, electric discharging rate and other factors (Eq. 26). The storage battery was supplied by Silvex Exports Pvt. Ltd, Mumbai, India. A solar charge controller regulates the supply of electric power from the PV module to the storage battery.

The thermoelectric module (TEM) is a solid-state heat pump that builds hot and cold sides when electric current flows across the module. The TEM converts the solar direct current (DC) to alternate current (AC) power. A thermoelectric module (model: TEC1-12705S, make: Hebei) was used in this study. Two heat sinks, one (size: 10×10×3 cm) at the hot side and the other (size: 4×4×2.6 cm) at the cold side of the TEM, were fixed. Besides, two low power consumption fans (3 W), one at the backside of the hot side heat sink and the other at the cold side heat sink, were fixed as shown in Fig. 1. This complete thermoelectric assembly was fixed onto the cooler box wall, as shown in Fig. 2. The heat sink at the hot side amplifies the heat transfer rate from the hot side of the TEM; thus, the heat will be dispelled outside of the cooler box; it also protects TEM from overheating and maintains an ambient environment. The heat sink at the cold side of the TEM facilitate in cool the cooling space. The cooling fans used to reject extra heat from the hot side of the TEM to the ambient environment, better ventilation and maintain the TEM's effectiveness. Fig. 2 shows the schematic diagram of the experimental setup.

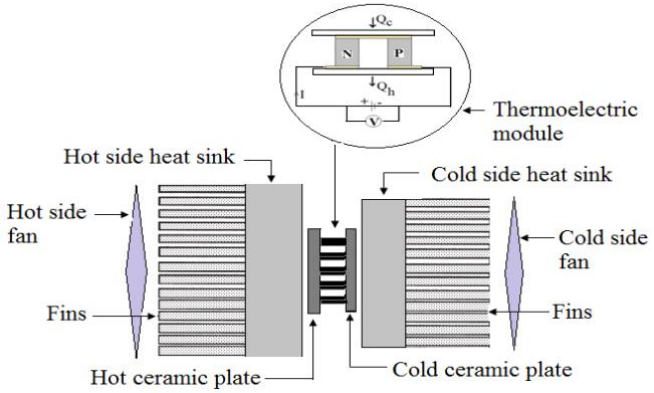

Fig. 1. Schematic arrangement of basic components of the thermoelectric cooling system.

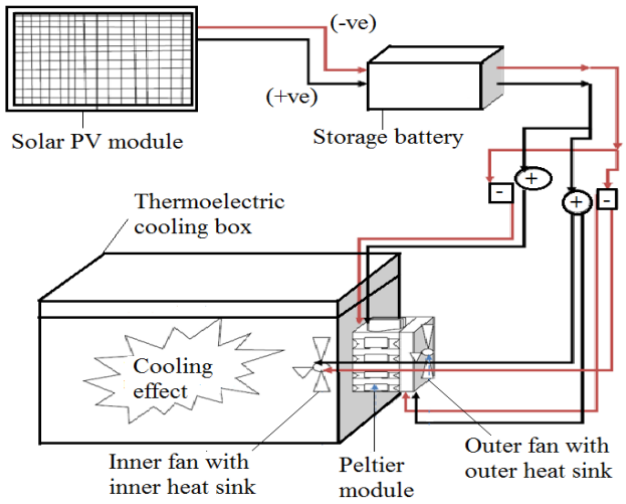

Fig. 2. Schematic diagram of the experimental portable solar thermoelectric cooler.

2.3. Text procedure

The solar-PV module was fixed with the required angle (40º) to receive maximum solar radiation incidence on the module. The PV module was connected to the solar charge controller, which connected with battery terminals using respective cables. The TEM was connected to the storage battery so that the red wire of the TEM connected with a positive power supply and the black wire with a negative power supply. The positive side of the TEM turns into the cold side of the TEM due to the absorption of heat, which is transferred to the other side, which became the hot side. The TEM's cold side was fixed inside the cooler box and the hot side of the TEM installed outside of the cooler box (Fig. 2). To evaluate the cooling performance of the STEC, power generation of PV module, the temperatures of hot and cold

sides of the TEM, power consumption, cooling capacity and COP were estimated. The power output of the PV module, current and voltage were measured using a digital multimeter, which connected with the PV module in parallel to measure the voltage and serially to measure the PV module's current rating. The temperatures of the cold side and hot side of the TEM were measured using T-type thermocouples wires. The thermocouples connected to the hot and cold sides of the TEM and other ends were connected with a digital temperature indicator with a resolution of 0.1ºC. The lab room temperature also recorded during the experiment. The voltage, electric current and power consumption of the STEC were measured using a digital energy meter. A data logger was used for logging the experimental data.

2.4. Methodology of the experimental analysis

In scientific studies on the solar-powered thermoelectric cooling system, calculations of total heat gain of the cooler box, COP of the thermoelectric module, and size of the solar-PV module are the most important factors.

2.4.1. Total heat gain of cooler box

The cooling process is a function of heat transfer through the walls of the cooler box, product heat, heat given off by fan and heat due to air-infiltration into the cooler. The average outside temperature during the work was taken for heat calculation since outside temperature varies with time. The heat loss through the wall of the cooler box (Q_w) was estimated using the following formula [24]:

$$Q_w = A_c U(T_0 - T_i) \quad (1)$$

$$U = \frac{1}{\frac{1}{h_{in}} + \frac{X_p}{K_p} + \frac{X_i}{K_i} + \frac{1}{h_{out}}}$$

The conduction heat loss (Q_m) inside the thermoelectric module can be estimated as [20,27].

$$Q_m = \frac{K_m A_m (T_h - T_c)}{X_m} \quad (2)$$

The product heat (Q_p) in the cooler can be determined as the method described by Gökçek and Şahin [24]. The product heat refers to the heat given off by the stored product. In this study, 0.5 kg fish fillets was kept in the solar thermoelectric cooler as product material. The specific heat capacity of the fish fillets about 3.85 kJ/kg K [28].

$$Q_p = \frac{M_p C_p (T_{pi} - T_{pf})}{3.6\,\Delta t} \quad (3)$$

The rated power consumption of the fan (Q_f) was used to calculate the heat given off by the fan at cold side of the TEM [20,24].

$$Q_f = N_f F_r \quad (4)$$

The heat due to infiltration of air into the cooler box by opening the top lid can be estimated as [29]:

$$Q_i = \frac{C_a E_b V_b (T_0 - T_i)}{3.6} \quad (5)$$

The total heat energy (Q_T) was calculated by adding the heat flow entering the cooler box, conduction heat loss inside the thermoelectric module, product heat, heat given off by the fan and air-infiltration heat. The total heat energy measured in watt.

$$Q_T = Q_w + Q_c + Q_p + Q_f + Q_i \quad (6)$$

2.4.2. Thermoelectric heat balance analysis

In general, Peltier heating, Peltier cooling, Joule heat, and Fourier heat are considered in the cooling and heating processes of thermoelectric system [5], and these are expressed in watt. A steady-state energy equilibrium model as described by Riffat and Ma [30] was applied to characterise the theoretical performance of the thermoelectric module.

The heat transferred at cold side of the TEM (Peltier cooling) was calculated using following expression [30]:

$$Q_{pc} = \alpha I T_c \quad (7)$$

The heat transferred at hot side of the TEM (Peltier heating) was estimated by following formula [5]:

$$Q_{ph} = \alpha I T_h \quad (8)$$

According to the Ohm's law, TEM generates Joule heat when current flow through it due to electrical resistance (R). Of which, 50% heat moved to the cold side and 50% heat moved to the hot side to balance the Joule heat [30]. The rate of Joule heating (Q_j) at the cold side or hot side can be estimated as:

$$Q_j = 0.5 I^2 R \quad (9)$$

The heat conduction (Fourier heat) from the cold side to the hot side through the thermoelectric material that subjected to the temperature gradient is given by [27]:

$$Q_k = K(T_h - T_c) = K\Delta T \quad (10)$$

The quantity of heat pumped by the TEM or absorbed at cold side of the TEM, i.e., the cooling capacity (Q_c), can be estimated by considering the heat balance Eqs. (7), (9) and (10):

$$Q_c = \alpha I T_C - 0.5 I^2 R - K\Delta T \quad (11)$$

The amount of heat transferred at the hot side of the TEM (Q_h) can be calculated by taking into account heat balance Eqs (8), (9), and (10):

$$Q_h = \alpha I T_h + 0.5 I^2 R - K\Delta T \quad (12)$$

The electrical power consumption of the TEM (P_{tm}) can be estimated by taking a difference in heat absorption and heat rejection at cold and hot sides of the TEM respectively as per the first law of thermodynamics [4,5,30]:

$$P_{tm} = Q_h - Q_c = I^2 R + \alpha I (T_h - T_c) \quad (13)$$

The electrical power consumption of the experimental thermoelectric cooler (P_c) was estimated by adding the power consumption of the TEM and fans [2,5,20,24].

$$P_c = n_{tm} P_{tm} + n_f P_f \quad (14)$$

As the heat energy in the cooled space of the thermoelectric cooler is absorbed at the cold side of the TEM during the cooling process, either Q_T or Q_c can be applied to estimate the coefficient-of-performance (COP) of the thermoelectric cooler [24]. The COP of the experimental thermoelectric cooler in the cooling mode was estimated as [4,5,24]:

$$COP = \frac{Q_c}{P_c} \tag{15}$$

Optimum electric current input to the TEM for maximum possible COP of the thermoelectric material exists when hot and cold side temperatures are steady-state. The electric current input can be determined as follows [16]:

$$I = \frac{V - \alpha \Delta T}{R} \tag{16}$$

2.4.3. Thermoelectric module's properties

As the values of TEM's properties such as electrical resistance (R), thermal conductance (K) and Seebeck coefficient (α) are not provided by the manufacture, a method described by Zhao and Tan [2] and Chen and Snyder [31] was applied to determine these properties as follows. The technical specifications of the TEM used in this study are presented in Table 1.

$$R = \frac{2(T_h - \Delta T_{max})^2}{T_h^2} \frac{Q_{max}}{I_{max}^2} \tag{17}$$

$$K = \frac{(T_h - \Delta T_{max})^2}{T_h^2} \frac{Q_{max}}{\Delta T_{max}} \tag{18}$$

$$\alpha = \frac{(T_h - \Delta T_{max})}{T_h^2} \frac{Q_{max}}{I_{max}} \tag{19}$$

The number of TEM required (n_{tm}) to pump the heat from the thermoelectric cooler depends on the refrigeration load (Q_T) of the cooler and the amount of heat pumped by the TEM (Q_c), which determined as [32]:

$$n_{tm} = \frac{Q_T}{Q_c} \tag{20}$$

2.4.2. Size of the solar-PV system

The solar-PV module generates the required electrical power to drive the solar thermoelectric cooler. Therefore total power needed from the PV module is about 1.2 times the actual power requirement (P_c) of the thermoelectric cooler (20% for DC-AC converting efficiency about 90% and power for recharge storage battery).

$$P_{pv} = P_c \times 1.2 \tag{21}$$

The daily electrical power production of a PV-module based on the annual average hourly radiation can be described as follows [33]:

$$P_{pv} = A_{pv}\, R_{pv}\, F_{pv}\, \frac{S_i}{S_{i-STC}}\, \frac{1}{t_s} \tag{22}$$

The nominal power output of the PV module was obtained by rearranging the Eq. (23) and denoted as Watt-peak (W_p).

$$R_{pv} = \frac{P_{pv}\, t_s}{A_{pv}\, F_{pv}} \frac{S_{i\_STC}}{S_i} \tag{23}$$

The annual average solar insolation (S_i) at the experimental location (Birbhum district of West Bengal, India) is 4.82 kWh/m^2/day [34]. The efficient sunshine time (t_s) for power generation in a day, derating factor (F_{pv}) and area (A_{pv}) of the PV module are assumed to be 5 h, 75% and 1 m^2, respectively.

The power output rating of experimental PV module can be obtained from the theoretical power output rating (Eq. 24). Therefore, a PV module size of 100 W_p is sufficient to meet the required power generation. The physical and electrical specifications of the PV module used in this study are presented in Table 1.

The batteries must supply sufficient electrical energy to drive the thermoelectric cooler when there is no sunshine. Thus, the battery capacity should be large enough to store energy. A method described by Dai et al. [16] was used to estimate the storage battery capacity (B_c) as follows:

$$B_c = \frac{P_c \times d_s}{\Phi_b \times \eta_b \times \delta \times (1 - \chi_b)} \tag{24}$$

The values of different parameters used in battery capacity calculation are given in Table 1.

Table 1. Specifications of the solar PV module (Vinova Energy Systems, India) and thermoelectric module (Hebei, China)

Solar PV module		Thermoelectric module		Battery parameters	
PV module type	VE12100	TEM type	TEC1-12705S	P_c	53.5 W
Maximum rated power (W_p)	100 W_p	I_{max}	5.3 A	Φ_b	0.85
Maximum power voltage (V_{mp})	18.58 V	U_{max}	15.4 V	η_b	0.90
Maximum power current (I_{mp})	5.98 A	$Q_{max.}$@ΔT=0	57 W	δ	0.90
Open circuit voltage (V_{oc})	22.58 V	ΔT_{max}	67 ºC	χ_b	0.05
Short circuit current (I_{sc})	5.96 A	T_h	40 ºC	d_s	1 day
Module efficiency (η_m)	13.2 %	N-P junction	127 couples		
Output tolerance	5 %	Max. temperature	138ºC		
Maximum series fuse rating	10 A	Dimension	40×40×3.8 mm		
Operating temperature	- 40 to 85 ºC	Design	Silicone sealed		
Module dimension	1032×672 mm	Material	Bismuth telluride		
Weight	8 kg	Weight	29 g		

PV module at standard test condition: solar irradiance 1.0 kW/m^2; module temperature 25°C; wind speed 1.0 m/s.

3. Results and Discussion

3.1. Power generation of PV module

Fig. 3(a) shows the variations in voltage and electric current of the solar-PV module during the experiment. As shown, an increasing trend in electric current and voltage of the PV module was observed from morning hours to noon hours, reached maximum levels at noon hours thereafter decreasing trend was observed. These increasing and decreasing trends occurred due to increasing and decreasing solar radiation intensity from morning hours to afternoon hours. The maximum current and voltage were 5.38 A and 16.34 V, respectively, at noon hours.

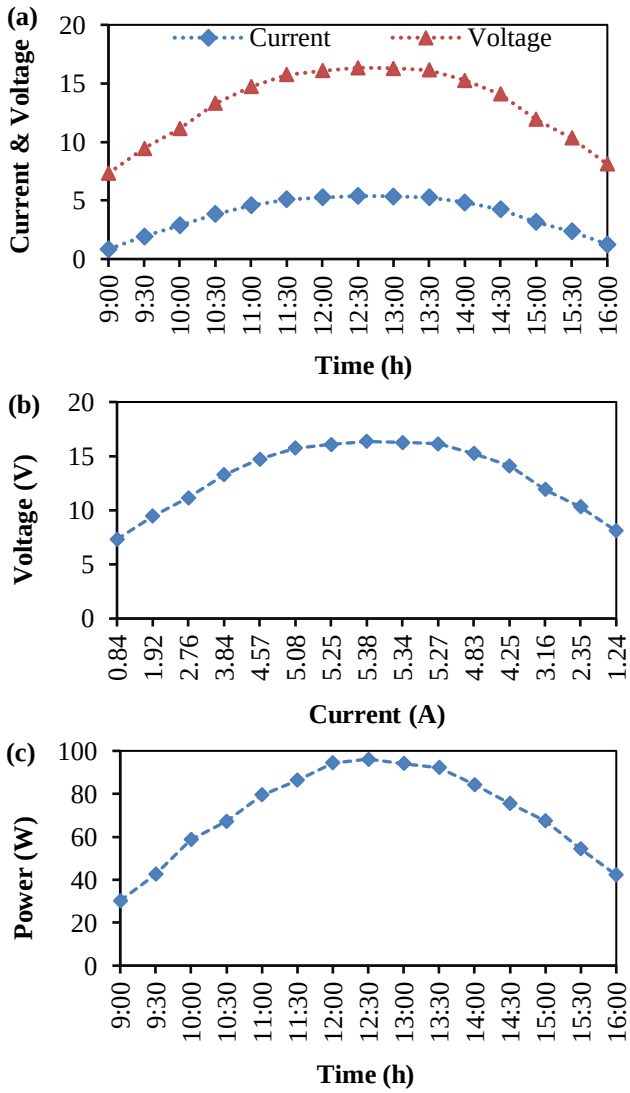

Fig. 3. Performance of solar-PV module during experiment (a) changes in voltage and electric current with time (b) voltage versus electric current (c) power generation by PV module with time.

Fig. 3(b) demonstrates the voltage changes against the solar-PV module's electric current during the experiment. As indicated, the voltage increased while increasing the electric current due to the increase in solar radiation intensity; however, the voltage decreased with decreasing electric current. The result indicates that the voltage is directly proportional to the electric current. The maximum voltage of 16.34 V observed at a maximum current of 5.38 A.

Fig. 3(c) presents the changes in power generation of solar-PV module during the experiment time. As shown, the PV module's power generation increased while increasing the solar radiation intensity whereas decreased while decreasing the intensity of solar radiation. Obviously, the power generation of the PV module depends on the solar radiation intensity. The maximum electrical power of 92-96 W observed at noon hours during the test period.

3.2. Experimental evaluation of solar thermoelectric cooler

The cooling capacity (see Eq. 11) and power consumption of the TEM (see Eq. 13) are mainly depends on the electric current input, hot and cold sides temperature difference, electrical resistance, thermal conductance and Seebeck coefficient of the TEM. The calculated values of R, K and α were 1.9886 Ω, 0.4107 W/K and 0.1882 V/K, respectively.

Fig. 4(a) shows the temperature variations in the thermoelectric module's cold side and outdoor (lab room) without a cooled item. The cold side temperature decreased rapidly from 30ºC to 14.4ºC at the first 30 min; subsequently, it reduced gradually and reached to 5±0.2ºC in 120 min thereafter, with no much significant reduction in temperature. On the other hand, no significant change in outdoor temperature was observed. The voltage is maintained at 12 V.

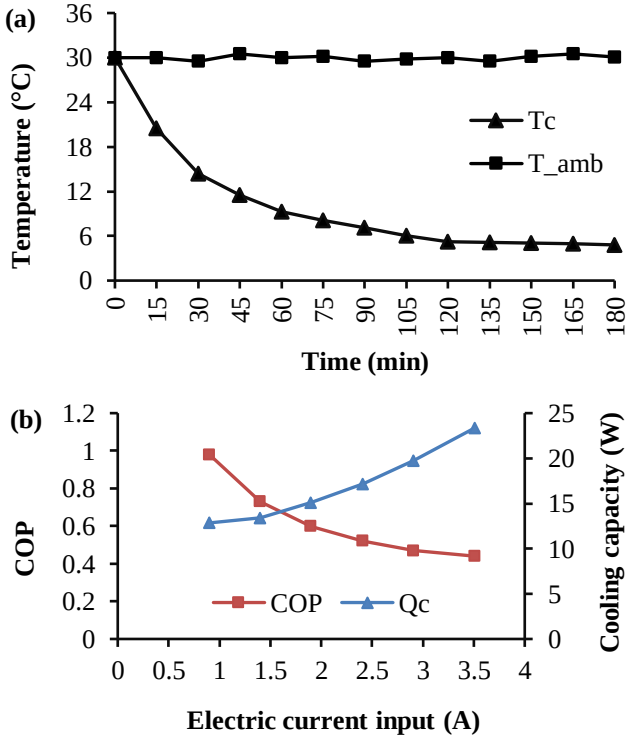

Fig. 4. Performance of the solar thermoelectric cooler during experiment without product load (a) temperature variations over the time (b) variations of COP and cooling capacity against electric current input.

Fig. 4(b) indicates the effect of electric current input on cooling capacity and COP of the STEC. The results showed that increasing electric current input results in decreasing the COP of the STEC. This is due to raising the electric power consumption of the TEM while increasing the electric current input, and therefore decreasing the COP of the STEC (See Eq. 15). On the other hand, the cooling capacity increased while increasing the electric current input. This is due to the increases the flow of electrons within the TEM and decreases the cold side temperature, thus increasing the cooling capacity of the TEM. It is observed that the cooling capacity increases from 12.9 W to 23.4 W, and the COP decreases from 0.98 to 0.44 by increasing the electric current input from 0.9 A to 3.5 A. The maximum cooling capacity of 23.4 W and the COP of 0.44 were observed at the electric current input of 3.5 A.

Fig. 5(a) describes the temperature variation of the thermoelectric module's cold and hot side with the loaded item. To test the cooling performance of the thermoelectric cooler, about 0.5 kg of fish fillets kept in the cooler. It can observe from the Figure that the cold side temperature (T_c) decreased to 5±0.2ºC in 180 min, and the hot side temperature (T_h) increased to 40.2°C. Besides, the temperature of fish fillets dropped to 6.5°C. It is also absorbed that the temperatures continued till the end of the experiment.

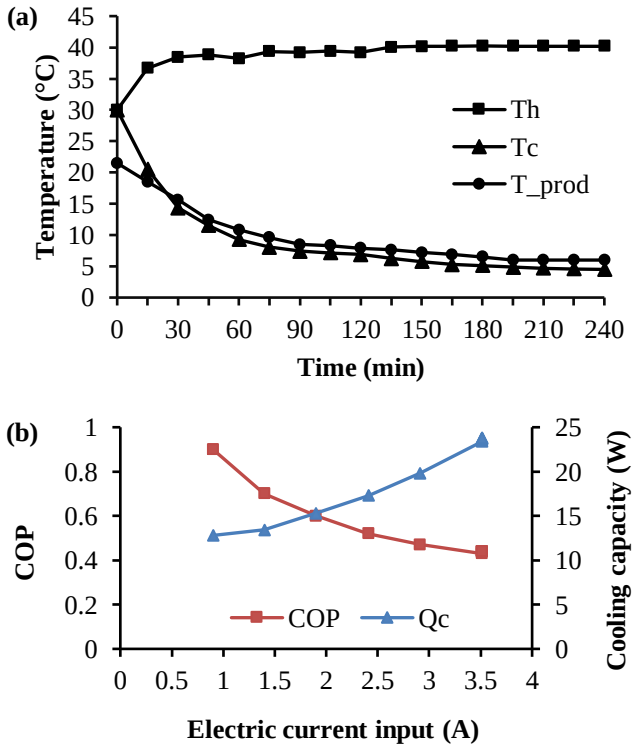

Fig. 5. Performance of the solar thermoelectric cooler during experiment with product load (0.5 kg fish fillets) (a) variations in temperature of product, hot and cold sides of the TEM (b) variations of COP and cooling capacity against electric current input.

Fig. 5(b) shows variations of the cooling capacity and COP of the STEC with product load (0.5 kg fish fillets) against electric current input. The result indicates that no significant changes in the cooling capacity and the COP of the STEC have either product load or no product load. However, to achieve this condition, the system with product load took about 180 min, whereas the system without load took around 120 min. It is clearly noticed from the Figure that the cooling capacity increased from 12.85 W to 23.8 W whereas decreased the COP from 0.98 to 0.44 by increasing the electric current input from 0.9 to 3.5 A.

As shown in Figures 4(b) and 5(b), the COP of the STEC greatly depends on the cooling capacity and electric current. The cooling capacity increased as the current consumption increases, whereas decreased the COP. Therefore, it is a big challenge in selecting the input current that maximises both cooling capacity and COP. A greatest COP of 0.98 obtained with a limited cooling capacity of 12.85 W at an electric current of 0.9 A.

Variations in current input according to voltage during the study are presented in Fig. 6. Obviously, the current input to the TEM is directly proportional to the voltage. The experiment observed that the voltage was raised to 12-13 V and the electric current flow also raised to about 3.5 A.

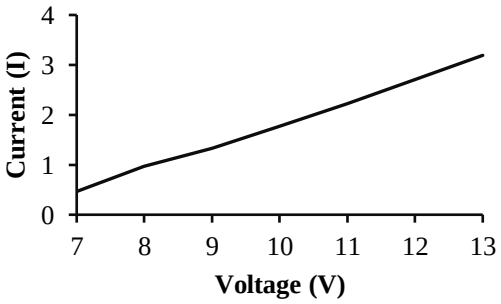

Fig. 6. Changes in electric current according to voltage

3.3. *Battery power*

The STEC was operated for a period of about 5-6 h after the sunset. The sunset times varied from 18:09 to 18:38 during the study period. The store electrical power in the battery exploited to drive the cooler during this time. The changes in the temperature of the TEM's cold and hot side were observed during this time. The temperature at the cold side was maintained at about 5ºC in the period and thereafter increased gradually. The electric current flow while using battery power was 3.5 A.

3.4. *Theoretical evaluation*

Fig. 7(a) demonstrates the thermoelectric module's cooling capacity at different hot and cold side temperature differences and electric current input. It is clearly seen from the Figure that the cooling capacity of the module increased with increasing electric current input and as well increased with increasing difference in temperature between the cold and hot sides of the TEM (ΔT). Moreover, the hot and cold side's temperature of TEM fluctuated by a change in the electric current input and voltage. Therefore, the cooling capacity of the TEM depends on the ΔT and amount of electric current input. A maximum cooling capacity of 7.2 W,

12.6 W, 17.9 W and 23.3 W was observed at the temperature difference of 20°C, 25°C, 30°C and 35ºC, respectively, electrical current flow of 3.51 A.

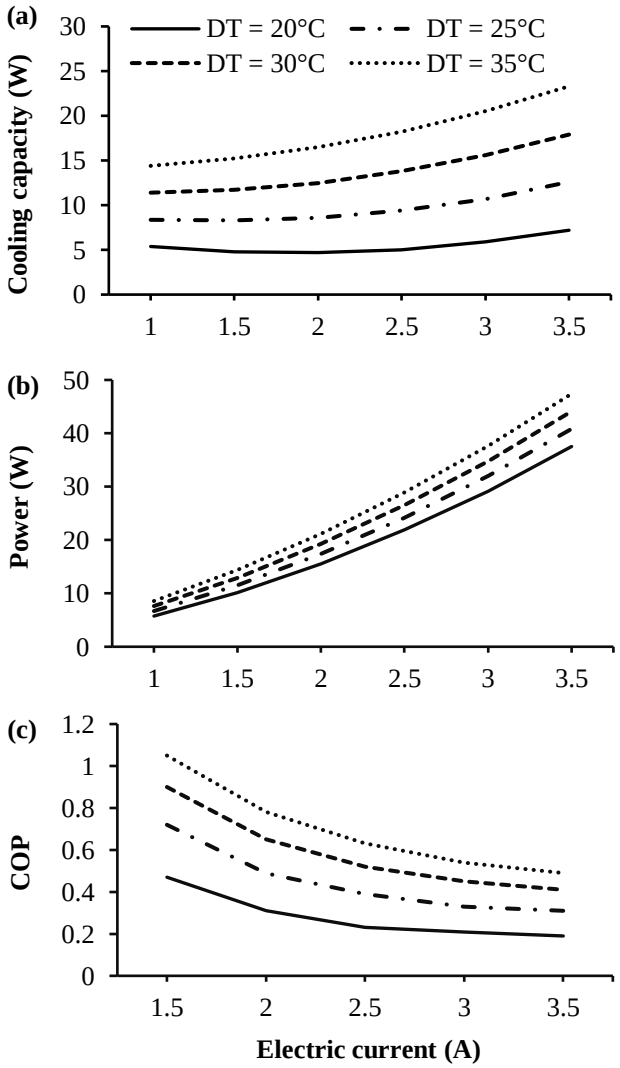

Fig. 7. Theoretical performance (a) Cooling capacity (b) Power consumption (c) Coefficient of performance (COP) of the thermoelectric module at temperature differences (ΔT) between hot and cold side.

Fig. 7(b) shows the power consumption of the thermoelectric module at different hot and cold side temperature differences and electric current input. The results showed that the power consumption increases while increasing the temperature difference between hot and cold sides and increases the electric current flow. It indicates that the thermoelectric module consumes more electrical power for the cooling process, reducing the temperature in the cooled space. The highest power consumption of 37.5 W, 40.8 W, 44.1 W and 47.4 W was recorded at temperature difference of 20°C, 25°C, 30°C and 35°C, respectively with an electric current of 3.5 A. Therefore, the power consumption of the thermoelectric module for cooling depends on the temperature difference between hot/cold sides and electric current.

Fig. 7(c) demonstrates the coefficient of performance of the thermoelectric module. The results showed that the COP decreased with increasing the amount of electric current. This may be due to the generation of more Joule heat at a higher electric current, which will balance the thermoelectric cooling effect. Joule heat could rise gradually as the electric current increases; therefore, a converging trend exhibited in the curves. However, the COP increased with increasing temperature difference at a given point of electric current. The result also demonstrated that the COP decreased while absorbing more heat and decreased energy consumption. Therefore, determining the best-balanced point for cooling capacity and COP is a principal component of the thermoelectric cooling system's optimization process.

In this study, a maximum theoretical cooling capacity of 23.3 W achieved at hot and cold sides temperature difference of 35°C with an electric current value of 3.5 A. The power consumption of the module was 47.4 W, and the COP of the system was found to be 0.49.

The results of present study have been compared with the findings of the various published works on solar PV driven thermoelectric refrigeration systems, and the consolidated findings of the present work and the previous works are presented in Table 2. Among portable thermoelectric refrigerator, the present designed STEC has a significant higher cooling capacity and COP.

The total weight and expected cost of the designed STEC are presented in Table 3. The expected execution cost of the STEC is 14243 INR or 196.6 USD, and its total weight is around 26 kg. It is concluded that the proposed STEC is a portable, cost-effective and perfect option to store the perishable foods in remote and rural areas where a consistent electrical power supply is not available.

4. Conclusion

In this work, a thermoelectric cooler driven by solar-PV module was fabricated and studied its cooling performance under the hot weather conditions. The total heat energy of the cooler box, sizing of the PV system, and battery capacity were also estimated. The temperature variations, cooling capacity, power consumption and COP of the STEC were investigated. The temperature of cooler decreased to 5±0.2ºC in 120 and 180 min for without and with load respectively. The cooling capacity of the STEC increases while increasing the electric current input, whereas a decreasing trend was observed in the COP. A minimum cooling capacity of 12.85 W and a maximum COP of 0.98 obtained at a minimal electric current input of 0.9 A. However, in a design point, the cooling capacity and power consumption of the STEC were 23.8 W and 53.5 W, respectively, in which the COP was found to be 0.44. Besides, the battery power utilized to drive the STEC for 5-6 h after sunset. The proposed STEC could be an alternate "green-option" to the domestic vapour compressor refrigerator in remote and rural areas where electricity is not accessible with additional benefits such as no moving parts, refrigerants free, active adaptability, comport, portable, does not required conventional electricity and low-cost application.

Table 2. A comparison of the present work with different previous works on the solar PV driven thermoelectric cooling systems

Authors	Refrigerator type and applications	Methodology	Findings			
			Power (W)	Cooling (W)	COP	Variations in temperature
Aboelmaaref et al. [5]	Solar thermoelectric air-conditioner for room air-conditioning (room size: 1.0 m^3)	The solar-PV system was integrated with a cooling unit which consists of 16 identical TEMs and 6 rectangular fin heat sinks	2.5 A	30	2.2	A cooling capacity of 30 W and the COP of 2.2 was obtained at a design point with an input current of 2.5 A, which suitable for save energy.
Chen et al. [7]	Solar thermoelectric chiller for water cooling.	The solar panel was used to drive thermoelectric chiller, where cold side of TEM was connected to the water tank.	16.7	12.2	0.74	The temperature of water drops from 18.5ºC to 14ºC and maintained the cooling capacity of 12.2 W.
Daghigh and Khaledian [8]	Solar thermoelectric cooling-heating system for water cooling.	The PV collector was used for thermoelectric cooling system, where 4 TEMs were connected to the water tank.	7911 kJ	N/A	5.4	They observed hot and cold side temperatures of TEM were 69 and -3°C, respectively.
Dai et al. [16]	Solar thermoelectric refrigerator for cold storage of vaccine, food and drink.	Solar-PV panel was connected to the refrigerator, which consists of TEM, heat sinks, storage battery and AC rectifier.	48-52	12-26	0.25-0.50	The cold side and water temperature dropped to 5°C and 10°C, respectively in 3 h and cooling production was 12 W at the end.
Abdul-Wahab et al. [20]	Portable solar thermoelectric refrigerator for domestic purpose (23 × 18 × 32 cm)	Solar PV cells were connected to a set of 10 TEMs. Each module consumed maximum power of 9.5 W.	95	15.33	0.16	The temperature was reduced from 27ºC to 5ºC in 44 min without load, and from 26ºC to 4ºC in 50 min with load (0.5 L canned drink)
He et al. [22]	Solar thermoelectric cooling system for room cooling (size: 0.125 m^3)	The solar cells were connected with thermoelectric device, heat exchanger and water tank which installed in an experimental room.	36	19.7-20.9	0.45	The room temperature was reduced to 17ºC. The COP of 0.45 was obtained with thermal and electrical efficiency of 12.06 and 10.27%, respectively.
Atta [25]	Solar thermoelectric cooler for room cooling (size: 30 m^3)	Solar PV system was connected to 30 TEMs which placed in closed loop liquid cooling system	4368	3150	0.72	A closed room space of 30 m^3 cooled to 14°C within 90 min when the PV input current at 11.2 Å and 12 V.
Present work	Portable solar thermoelectric cooler for storage of perishable foods (size: 0.0252 m^3)	Solar PV system was connected with the TEC, which consist of TEM, heat sink-fan. The PV and store battery power were utilized in day and night time, respectively.	53.5	23.8	0.44	The cold side temperature decreased to 5±0.2ºC in 180 min and hot side temperature increased to 40.2°C. Besides, the temperature of fish fillets dropped to 6.5°C.

Table 3. The weight and expected execution cost of the designed solar thermoelectric cooler

Items	Dimensions	Weight (kg)	Qty	Cost (INR)	Cost (USD)
HDPE cooler box	0.36 × 0.28 × 0.25 m	2.29	1	1299.0	17.93
Solar PV panel	1032 × 672 mm	8.0	1	3845.0	53.08
Storage battery	80 Ah	15.0	1	1800.0	24.85
PV charge controller	12 V, 30 A	0.16	1	1099.0	15.17
Peltier module	40 × 40 × 3.8 mm	0.029	1	500.0	6.90
Outer heat sink	10 × 10 × 3 cm	0.42	1	850.0	11.73
Inner heat sink	4 × 4 × 2.6 cm	0.012	1	450.0	6.21
Sink fans	3 W	0.1	2	900.0	12.42
Miscellaneous				3500.0	48.31
Total		26.01		14243.0	196.6

Acknowledgements

The authors acknowledge financial support from the Department of Science and Technology, Government of India (No: DST/INSPIRE Fellowship/IF170433 Dated: 10 January 2018). The authors wish to thank the Department of Agricultural Engineering, Visva-Bharati, West Bengal, India and the Faculty of Fishery Science, West Bengal University of Animal & Fishery Sciences, India for laboratory facilities and immense technical supports.

Nomenclature

A_c	Area of the cooler walls, m^2	n_f	Number of fans
U	Overall heat transfer coefficient, W/m^2K	F_r	Rating of fan, W
T_0	Average outside air temperature, °C	Q_{pc}	Peltier cooling rate, W
T_i	Inside temperature of cooling chamber, °C	Q_{ph}	Peltier heating rate, W
K_p	Thermal conductivity of HDPE wall, W/mK	Q_j	joule heating rate of the TEM, W
K_i	Thermal conductivity polyurethane foam, W/mK	Q_k	heat conduction between cold/hot end of TEM, W
X_p	Thickness of HDPE wall, m	Q_c	quantity of heat absorbed at cold end of TEM, W
X_i	Thickness of insulating material, m	Q_h	quantity of heat transferred at hot side of TEM, W
K_m	Thermal conductivity of Bismuth telluride, W/mK	P_{tm}	electric power consumption of the TEM, W
A_m	Cross-sectional area of the TEM, m^2	P_c	power consumption of experimental TEC, W
E_b	Number of times the cooler air exchanged per day	COP	coefficient-of-performance of the TEC
V_b	Internal volume of the cooler box, m^3	I	Electrical current, A
K	Thermal conductance of TEM material, W/K	R	Electrical resistance of TEM, Ω
X_m	Thickness of length of the TEM, m	I_{max}	Maximum input electric current to the TEM, A
T_c	Temperature at cold side of the TEM, °C	P_{pv}	Daily energy production of a solar-PV module, W
T_h	Temperature at the hot side of the TEM, °C	A_{pv}	Area of PV module to receive solar irradiation, m^2
M_p	Mass of the fish fillets, kg	F_{pv}	Solar-PV module derating factor, %
C_p	Specific heat capacity of the fish product, kJ/kg K	R_{pv}	Power output rate of PV module under STC, W_p
T_{pi}	Initial temperature of fish product, ºC	S_{i_STC}	Solar incident radiation at STC, kW/m^2
T_{pf}	Final temperature of fish product, ºC	t_s	Efficient sunshine time for power generation, h
C_a	Specific heat of the humid air, 1.3 kJ/m^3°C	d_s	Power supply duration without sunshine, day
Q_{max}	Maximum heat absorbed at cold side of the TEM when I_{max} and $\Delta T_{max} = 0$	S_i	Solar insolation on the PV-module at the current time step, kW/m^2

Greek symbols

α	Seebeck coefficient of TEM, V/K	Δt	Time required to cool fish from T_{pi} to T_{pf}, h
Φ_b	Degree of electric discharging	η_b	Efficiency of the storage battery
δ	Correction coefficient of temperature	χ_b	Loss coefficient of battery current
ΔT	Hot and cold side temperature difference of the thermoelectric module, °C	ΔT_{max}	Maximum temperature difference between hot and cold side of the TEM at $Q_c = 0$, °C

References

[1] S. Jugsujinda, A. Vora-ud A, and T. Seetawan, "Analysing of thermoelectric refrigerator performance," Procedia Eng., vol. 8, pp. 154-159, 2011, doi: 10.1016/j.proeng.2011.03.028.

[2] D. Zhao, and G. Tan, "Experimental evaluation of a prototype thermoelectric system integrated with PCM (phase change material) for space cooling," Energy, vol. 68, pp. 658-666, 2014a, doi: 10.1016/j.energy.2014.01.090.

[3] L. Qia, H. Pana, X. Zhua, X. Zhanga, W. Salmana, Z. Zhanga, L. Lia, M. Zhub, Y. Yuana, and B. Xianga, "A portable solar-powered air-cooling system based on phase-change materials for a vehicle cabin," Energ. Convers. Manage., vol. 150, pp. 148-158, 2017, doi: 10.1016/j.enconman.2017.07.067.

[4] M. Mirmanto, S. Syahrul, and Y. Wirdam, "Experimental performances of a thermoelectric cooler box with thermoelectric position variations," Eng. Sci. Technol. Int. J., vol. 22, pp. 177-184, 2019, doi: 10.1016/j.jestch.2018.09.006.

[5] M. M. Aboelmaaref, M. E, Zayed, A. H. Elsheikh, A. A. Askalany, J. Zhao, W. Li, K. Harby, S. Sadek, and M. S. Ahmed, "Design and performance analysis of a thermoelectric airconditioning system driven by solar photovoltaic panels," Proc. IMechE Part C: J. Mech. Eng. Sci., vol. 234. no. 24, pp. 1-14, 2020, doi: 10.1177/0954406220976164.

[6] F. Afshari, "Experimental and numerical investigation on thermoelectric coolers for comparing air-to-water to air-to-air refrigerators," J. Therm. Anal. Calorim., vol. 144, pp. 855-868, 2021, doi: 10.1007/s10973-020-09500-6.

[7] Y. Chen, Z. Chien, W. Lee, C. Jwo, and K. Cho, "Experimental investigation on thermoelectric chiller driven by solar cell," Int. J. Photoenergy, article ID 102510, 2014, doi: 10.1155/2014/102510.

[8] R. Daghigh, and Y. Khaledian, "Effective design, theoretical and experimental assessment of a solar thermoelectric cooling-heating system," Sol. Energy., vol. 162, pp. 561-572, 2018, doi: 10.1016/j.solener.2018.01.012.

[9] M. Zeyghami, D. Y. Goswami, and E. Stefanakos, "A review of solar thermo-mechanical refrigeration and cooling methods. Renew," Sust. Energy Rev., vol. 51, pp. 1428-1445, 2015, doi: 10.1016/j.rser.2015.07.011.

[10] A. Harrouz, and O. Harrouz. "Application of solar energies to reinforce the flow water of foggara in the adrar region". Int. J. Smart Grid, vol.2, no.4, pp. 203-208, 2018.

[11] M.E. Shayan, and G. Najafi. "Energy-Economic optimization of thin layer photovoltaic on domes and cylindrical towers". Int. J. Smart Grid, vol.3, no.2, pp. 84-94, 2019.

[12] K.E. Okedu, A. Al Senaidi, I. Al Hajri, I. Al Rashdi, and W. Al Salmani. "Real time dynamic analysis of solar PV integration for energy optimization". Int. J. Smart Grid, vol.4, no.2, pp. 68-79, 2020.

[13] R. Wang, O.T. Tai, and K.W. Tam. "Solar radiation reduction monitoring of macao world heritage district photovoltaic system using GIS and UHF RFID obstacle detection approach" 9th International Conference on Smart Grid (icSmartGrid2021), Paper ID:39, Portugal, 29 June-01 July 2021.

[14] M. Colak, S. Balcı "Intelligent techniques to connect renewable energy sources to the grid: A review". 9th International Conference on Smart Grid (icSmartGrid2021), Paper ID:51, Portugal, 29 June-01 July 2021.

[15] R. Best, and N. Ortega, "Solar refrigeration and cooling," Renew. Energy., vol. 16, pp. 685-690, 1999. doi: 10.1016/s0960-1481(98)00252-3.

[16] Y. J. Dai, R. Z. Wang, and L. Ni, "Experimental investigation and analysis on a thermoelectric refrigerator driven by solar cells," Sol. Energ. Mat. Sol. C., vol. 77, no. 4, pp. 377-391, 2003, doi: 10.1016/S0927-0248(02)00357-4.

[17] D. Zhao, and G. Tan, "A review of thermoelectric cooling: Materials, modelling and applications," Appl. Therm. Eng., vol. 66, pp. 15-24, 2014b, doi: 10.1016/j.applthermaleng.2014.01.074.

[18] S. B. Riffat, S. A. Omer, and X. Ma, "A novel thermoelectric refrigeration system employing heat pipes and a phase change material: an experimental investigation," Renew. Energy., vol. 23, pp. 313-323, 2001, doi: 10.1016/S0960-1481(00)00170-1.

[19] G. Min, and D. M. Rowe, "Experimental evaluation of prototype thermoelectric domestic-refrigerators," Appl. Energy., vol. 83, pp. 133-152, 2006, doi: 10.1016/j.apenergy.2005.01.002.

[20] S. A. Abdul-Wahab, A. Elkamel, A. M. Al-Damkhi, I. A. Al-Habsi, H. S. Al-Rubai'ey, A. K. Al-Battashi, A. R. Al-Tamimi, K. H. Al-Mamari, and M. U. Chutani, "Design and experimental investigation of portable solar thermoelectric refrigerator," Renew. Energy., vol. 34, pp. 30-34, 2009, doi: 10.1016/j.renene.2008.04.026.

[21] T. C. Cheng, C. H. Cheng, Z. Z. Huang, and G. C. Liao, "Development of an energy-saving module via a combination of solar cells and thermoelectric coolers for green building applications," Energy, vol. 36, pp. 133-140, 2011, doi: 10.1016/j.energy.2010.10.061.

[22] W. He, J. Zhou, J. Hou, C. Chen, and J. Ji, "Theoretical and experimental investigation on a thermoelectric cooling and heating system driven by solar" Appl. Energy., vol. 107, pp. 89-97, 2013, doi: 10.1016/j.apenergy.2013.01.055.

[23] B. Ohara, R. Sitar, J. Soares, P. Novisoff, A. Nunez-Perez, and A. Lee, "Optimisation strategies for a portable thermoelectric vaccine refrigeration system in developing communities", J. Electron. Mater., vol. 44, pp. 1614-1626, 2015, doi: /10.1007/s11664-014-3491-9.

[24] M. Gökçek, and F. Şahin, "Experimental performance investigation of mini channel water cooled-thermoelectric refrigerator", Case Stud. Therm. Eng., vol. 10, pp. 54-62, 2017. doi: 10.1016/j.csite.2017.03.004.

[25] R. M. Atta, "Solar thermoelectric cooling using closed-loop heat exchangers with macro channels," Heat Mass Transfer., vol. 53, pp. 2241-2254, 2017, doi: 10.1007/s00231-017-1965-z

[26] J. Batra, V. Dabra, P. Sharma, and V. Saini, "Performance evaluation of thermoelectric refrigerator based on natural and forced mode of cooling processes", In: Saha P, et al. editors. Advances in fluid and thermal engineering, Singapore: Springer Nature, pp. 317-324, 2019, doi: 10.1007/978-981-13-6416-7_30.

[27] R. Bjørk, D. V. Christensen, D. Eriksen, and N. Pryds, "Analysis of the internal heat losses in a thermoelectric generator," Int. J. Therm. Sci., vol. 85, pp. 12-20, 2014, doi: 10.1016/j.ijthermalsci.2014.06.003.

[28] B. Margeirsson, H. L. Lauzon, L. Porvaldsson, S. V. Árnason, S. Arason, K. L. Valtýsdóttir, and E. Martinsdóttir, "Optimised chilling protocols for fresh fish", Matís Report, vol. 54. pp. 1-28, 2010.

[29] S. Akdemir, "Designing of cold stores and choosing of cooling system elements", J. Appl. Sci., vol. 8, no. 5, pp. 788-794, 2008.

[30] S. B. Riffat, and X. Ma, "Improving the coefficient of performance of thermoelectric cooling systems: a review", Int. J. Energy Res., vol. 28, pp. 753-768, 2004, doi: 10.1002/er.991.

[31] M. Chen, and G. J. Snyder, "Analytical and numerical parameter extraction for compact modelling of thermoelectric coolers", Int. J. Heat Mass. Trans., vol. 60, pp. 689-699, 2013, doi: 10.1016/j.ijheatmasstransfer.2013.01.020.

[32] O. Francis, C. J. Lekwuwa, and I. H, "Performance evaluation of a thermoelectric refrigerator", Int. J. Eng. Innov. Technol., vol. 2, no. 7, pp. 18-24, 2013.

[33] G. M. Masters, *Renewable and Efficient Electric Power Systems*, New Jersey: John Wiley & Sons, 2004.

[34] National Renewable Energy Laboratory, New Delhi. Green project support: solar irradiation-West Bengal, http://greenprojectsupport.blogspot.in/p/solar-irradiation-table.html [14 January 2021].